

## Peroxisome Proliferator-Activated Receptor $\gamma$ Controls *Muc1* Transcription in Trophoblasts

Tali Shalom-Barak,<sup>1</sup> Jill M. Nicholas,<sup>1</sup> Yongxu Wang,<sup>2</sup> Xiaowen Zhang,<sup>1</sup> Estelita S. Ong,<sup>2,3</sup>  
Timothy H. Young,<sup>1</sup> Sandra J. Gendler,<sup>4</sup> Ronald M. Evans,<sup>2,3</sup>  
and Yaacov Barak<sup>1\*</sup>

*The Jackson Laboratory, Bar Harbor, Maine<sup>1</sup>; Howard Hughes Medical Institute<sup>3</sup> and  
The Salk Institute,<sup>2</sup> La Jolla, California; and Department of Biochemistry and Molecular Biology,  
Mayo Clinic, Scottsdale, Arizona<sup>4</sup>*

Received 30 June 2004/Returned for modification 26 July 2004/Accepted 20 September 2004

**The nuclear receptor peroxisome proliferator-activated receptor  $\gamma$  (PPAR $\gamma$ ) is essential for placental development. Here, we show that the mucin gene *Muc1* is a PPAR $\gamma$  target, whose expression is lost in PPAR $\gamma$  null placentas. During differentiation of trophoblast stem cells, PPAR $\gamma$  is strongly induced, and *Muc1* expression is upregulated by the PPAR $\gamma$  agonist rosiglitazone. *Muc1* promoter is activated strongly and specifically by liganded PPAR $\gamma$  but not PPAR $\alpha$  or PPAR $\delta$ . A PPAR binding site (DR1) in the proximal *Muc1* promoter acts as a basal silencer in the absence of PPAR $\gamma$ , and its cooperation with a composite upstream enhancer element is both necessary and sufficient for PPAR $\gamma$ -dependent induction of *Muc1*. In the placenta, MUC1 protein is localized exclusively to the apical surface of the labyrinthine trophoblast around maternal blood sinuses, resembling its luminal localization on secretory epithelia. Last, variably penetrant maternal blood sinus dilation in *Muc1*-deficient placentas suggests that *Muc1* regulation by PPAR $\gamma$  contributes to normal placental development but also that the essential functions of PPAR $\gamma$  in the organ are mediated by other targets.**

Peroxisome proliferator-activated receptor  $\gamma$  (PPAR $\gamma$ ) is an orphan nuclear receptor with diverse biological activities of prime clinical importance (20). It heterodimerizes with RXR to regulate transcription of target genes through response elements (PPREs) comprised of direct repeats of a core motif spaced by 1 bp (underlined) (AGGTCANAGGTCAN; DR1) (15). PPAR $\gamma$  is the molecular target for the thiazolidinedione class of insulin sensitizers, which are widely prescribed for the treatment of type II diabetes (9). It is also a key regulator of adipocyte differentiation and regulates genes mediating lipid homeostasis pathways in adipocytes and macrophages (4, 6, 30). In addition, PPAR $\gamma$  has been implicated as a differentiation factor and a potential anti-oncogenic target in breast and colon cancer (27).

PPAR $\gamma$  deficiency results in death by the 10th day of gestation (E10.0) (3). At this developmental stage, PPAR $\gamma$  is expressed abundantly and exclusively in the placenta, and rescue of PPAR $\gamma$  null embryos to term by tetraploid chimeras shows that its essential functions are confined to the trophoblast (3). During placentation, structures transducing either maternal or fetal blood interdigitate to form a labyrinthine network of vessels. Histological studies reveal that PPAR $\gamma$  null placentas fail to form this vascular labyrinth (3). Fetal blood circulates in the placenta in endothelium-lined vessels that adhere intimately to the trophoblast. In PPAR $\gamma$ -deficient placentas, the tight interface between the trophoblast and the fetal endothelium is severely disrupted, and consequently, fetal vessels arrest at the chorionic plate. Once in the placenta, maternal blood leaves the arterial system and bathes the trophoblast through a series of small blood pools, or lacunae, that are lined

immediately by the labyrinthine trophoblast (2). These blood pools are dilated and torn in PPAR $\gamma$  null placentas, forming an abnormal, continuous blood sinus on the maternal side of the labyrinth, with overt phagocytosis of maternal erythrocytes by junctional zone trophoblasts (3). Normal labyrinthine trophoblast differentiates into a barrier epithelium that separates the maternal and fetal circulations while performing the essential exchange of metabolites between the two (7). This differentiation is critical for vascular remodeling, as demonstrated in various mouse mutants (21). However, the labyrinthine trophoblast of PPAR $\gamma$  null placentas fails to undergo typical morphological and cellular changes, such as compaction, syncytium formation, and lipid droplet accumulation (3). Embryos deficient for RXR $\alpha$ , alone or in combination with RXR $\beta$ , exhibit defects that are similar to those seen in PPAR $\gamma$  null placentas, demonstrating the functional dependency of PPAR $\gamma$  on RXR (22, 31).

Although the list of defects in PPAR $\gamma$  null placentas is extensive, no specific target genes have been established for these phenotypes. Here, an effort to identify and characterize transcriptional targets of PPAR $\gamma$  revealed that the mucin gene *Muc1* is a tightly regulated PPAR $\gamma$  target in the placenta and differentiated trophoblast stem cells. This regulation is mediated by the cooperative action of PPAR $\gamma$ -binding and non-binding elements in the proximal part of the *Muc1* promoter, whose protein product is confined to the trophoblast layer surrounding the maternal lacunae. This asymmetric distribution is analogous to the previously established localization of MUC1 protein on luminal surfaces of simple secretory epithelia (5) and implicates the maternal lacunae in the placenta as the anatomical analogues of secretory lumens. About half of *Muc1* null placentas exhibit dilation of the maternal lacunae, suggesting that *Muc1* may participate in this aspect of the PPAR $\gamma$  null phenotype. Our data provide new mechanistic insights into

\* Corresponding author. Mailing address: The Jackson Laboratory, 600 Main St., Bar Harbor, ME 04609. Phone: (207) 288-6704. Fax: (207) 288-6077. E-mail: ybarak@jax.org.

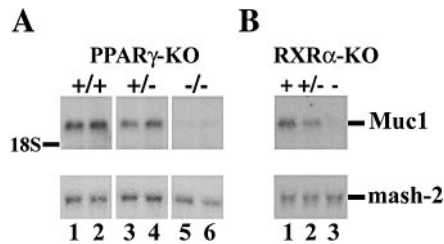


FIG. 1. PPAR $\gamma$  and RXR $\alpha$  are obligatory for placental *Muc1* expression. Northern blot analysis of RNA from pools of genotypically identical placentas at E9.5 reveals *Muc1* expression in wt placentas and its loss in both PPAR $\gamma$  (A) and RXR $\alpha$  (B) null placentas. Placentas heterozygous for either nuclear receptor (+/-) express roughly half the wt level of *Muc1*. A *Mash2* probe was used for quantitative normalization.

PPAR $\gamma$  action in trophoblasts, both by implicating it in shared biological regulation of epithelia and trophoblast and by revealing novel combinatorial interactions of PPAR $\gamma$  in target regulation.

#### MATERIALS AND METHODS

**Preparation of placental RNA.** Individual placentas were isolated from E9.5 embryo progeny of either PPAR $\gamma$ <sup>+/-</sup> (3) or RXR $\alpha$ <sup>+/-</sup> (28) breeder pairs and kept frozen at -80°C. The corresponding genotypes were determined by PCR of yolk sac DNA, as described previously (3), at which stage placentas with similar genotypes were pooled in groups of four, and RNA was extracted with Tri-Reagent. RNA preparations were further purified by treatment with RNase-free DNase and reextraction.

**RDA.** Total RNA (1  $\mu$ g) from either wild-type or PPAR $\gamma$ <sup>-/-</sup> placentas was converted to double-stranded cDNA, using the SMART PCR cDNA synthesis kit (Clontech). This cDNA was amplified through several rounds of long-range PCR, using Advantage *Taq* polymerase mix (Clontech). The amplified full-length cDNA was digested with DpnII and used to carry out reciprocal representational difference analysis (RDA) essentially as described previously (11), except that amplification of subtracted products was performed by using Advantage *Taq* polymerase mix and for 13 to 17 amplification cycles only. An additional modification was the supplementation of the subtracted driver cDNA population with Sau3AI-digested PPAR $\gamma$  (added to null driver) or *lacZ* and *neo* (added to the wild-type [wt] driver) to circumvent differential recloning of these genes. At the end of three rounds of subtraction-amplification, individual bands could be discerned on agarose gels, from which they were isolated and subcloned into pBluescript. Ten plasmid clones from each band were sequenced to determine its predominant composition, and sequences iterated more than once were subjected to BLAST analysis with the National Center for Biotechnology Information database to determine identity as well as being reprobated against RNA from PPAR $\gamma$ <sup>+/+</sup>, PPAR $\gamma$ <sup>+/-</sup>, and PPAR $\gamma$ <sup>-/-</sup> placentas to confirm true differentials.

**Trophoblast stem (TS) cell culture.** GFP-Trf mouse trophoblast stem cells (29) were cultured on a feeder layer of embryonic fibroblasts in RPMI 1640 medium containing 20% serum, fibroblast growth factor 4 (FGF4; 25 ng/ml; Sigma), and heparin (1  $\mu$ g/ml), with medium change every other day. Cells were passaged once in the absence of feeder cells in a similar medium supplemented with 70% embryonic fibroblast conditioned medium and then split for the various experiments. Differentiation was accomplished by withdrawing conditioned medium, FGF4, and heparin from the medium. Where appropriate, cultures were supplemented with 1  $\mu$ M rosiglitazone.

**Northern blots, EMSA, transfections, and reporter assays.** Northern blots and an electrophoretic mobility shift assay (EMSA) were carried out as described previously (3, 10). Supershift was performed using concentrated polyclonal  $\alpha$ -PPAR $\gamma$  (H-100) or  $\alpha$ -RXR $\alpha$  (D-20) antibodies (SantaCruz Biotech). Transfections of CV1 cells and reporter assays were carried out with a 48-well format as described previously (9), with some modifications. In short, wells containing 50 to 70% confluent CV1 cells were lipofected with the indicated plasmid combinations, using DOTAP (Avanti Polar Lipids, Inc.). Receptors, reporters, and cytomegalovirus (CMV)-*lacZ* controls were transfected at 25, 62, and 125 ng/well, respectively. Lipofection medium was replaced 3 to 5 h after transfection with Dulbecco's modified Eagle's medium containing 2% fetal calf serum and the indicated ligand combinations. Cells were extracted 24 to 36 h later and assayed for luciferase and  $\beta$ -galactosidase activities. Data shown reflect averages and standard deviations for normalized luciferase activity divided by  $\beta$ -galactosidase activity in triplicate wells from one

representative experiment out of at least four repeats with qualitatively similar results.

**Histology and immunofluorescence.** C57BL/6J *Muc1*<sup>+/-</sup> breeder pairs (26) were intercrossed, and pregnancies were timed by monitoring coital plugs. Embryos and placentas were retrieved from pregnant females at the indicated gestational day, and respective genotypes were determined by PCR of DNA from embryonic matter. For histology, placentas were fixed for 24 h in 10% formalin, embedded in paraffin, sectioned at 5  $\mu$ m, and stained with hematoxylin and eosin. For immunofluorescence, placentas were fixed overnight in Bouin's solution, washed with running water for 6 h, embedded in paraffin, and sectioned at 5  $\mu$ m. MUC1 was detected using a diluted hybridoma supernatant containing an Armenian hamster-derived monoclonal antibody against the short cytoplasmic tail (CT2) (S. J. Gendler, unpublished data) and secondary Cy3-conjugated goat anti-Armenian hamster antibody (10  $\mu$ g/ml; Jackson Immunoresearch). Caveolin-1 was detected by using a polyclonal rabbit antiserum (5  $\mu$ g/ml; Transduction Labs) and Alexa488-linked goat anti-rabbit antibody (5  $\mu$ g/ml; Molecular Probes, Inc.). All incubations and washes were carried out in phosphate-buffered saline containing 0.05% Tween 20 and 5% normal goat serum.

#### RESULTS

***Muc1* expression is lost in PPAR $\gamma$  null placentas.** To identify PPAR $\gamma$  target genes in trophoblasts, we screened for mRNA species enriched in wt versus PPAR $\gamma$  null placentas by using RDA (11). This screen identified the mucin-1 gene, *Muc1* (25). Northern blot analysis confirmed that *Muc1* is expressed in wt placentas at E9.5 (Fig. 1A, lanes 1 to 2, and 1B, lane 1) and is virtually absent from either PPAR $\gamma$  null or RXR $\alpha$  null placentas (Fig. 1A, lanes 5 and 6; Fig. 1B, lane 3, respectively). Moreover, placentas heterozygous for either

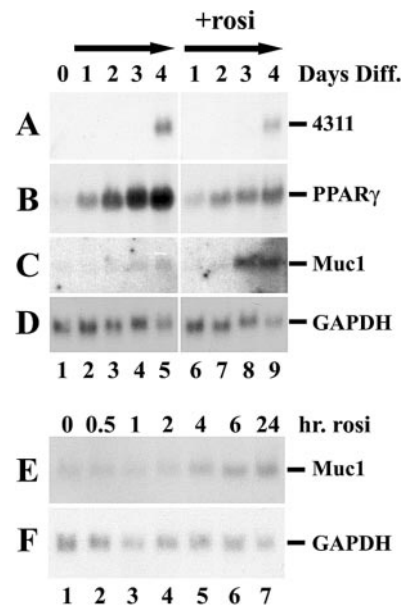


FIG. 2. PPAR $\gamma$  and *Muc1* induction during TS cell differentiation. (A-D) TS cells were grown continuously in the presence of FGF4 and embryonic fibroblast conditioned medium (lane 1) or induced to differentiate by factor withdrawal in the absence (lanes 2 to 5) or presence of 1  $\mu$ M of the PPAR $\gamma$  agonist rosiglitazone (+rosi; lanes 6 to 9). RNA was extracted at daily intervals after the onset of differentiation (top), and expression of the spongioroblast differentiation marker 4311 (A) and those of PPAR $\gamma$  (B), *Muc1* (C), and glyceraldehyde-3-phosphate dehydrogenase (GAPDH) (D) were analyzed by Northern blotting. (E-F) TS cells were induced to differentiate for 4 days and then treated with 1  $\mu$ M rosiglitazone for the indicated durations (top). Expression of *Muc1* (E) and glyceraldehyde-3-phosphate dehydrogenase (GAPDH) (F) was analyzed.

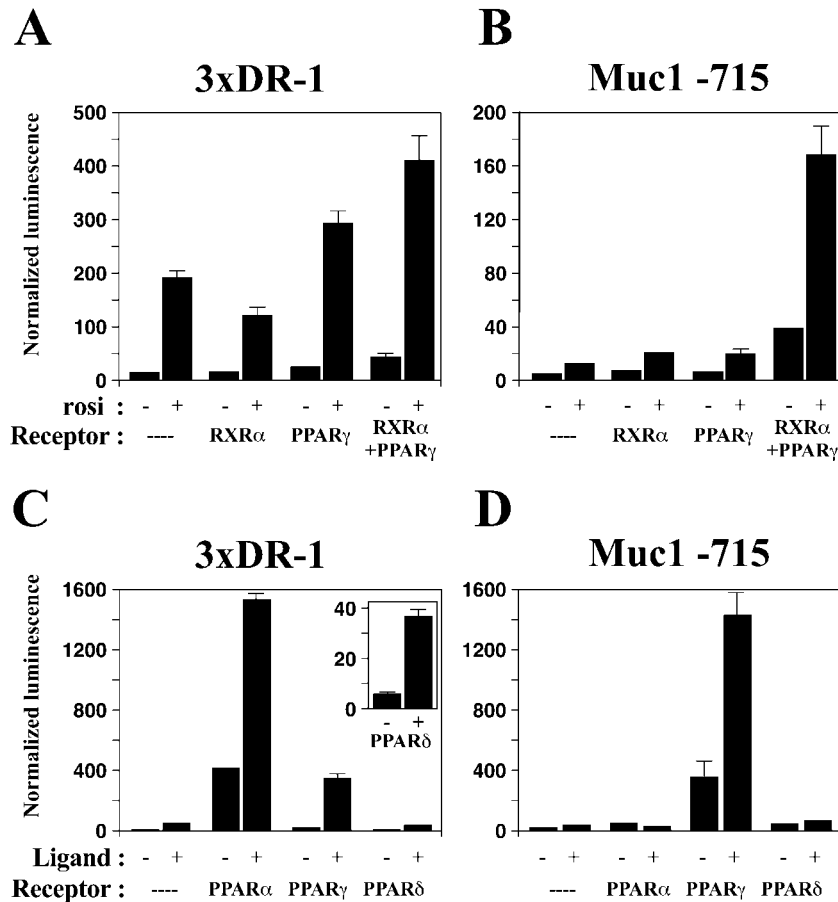


FIG. 3. Robust, PPAR $\gamma$ -specific activation of the *Muc1* promoter by PPAR $\gamma$ /RXR $\alpha$  heterodimers. CV1 cells were transfected with luciferase reporters driven by either a trimerized consensus PPRE sequence (3xDR-1) (A, C) or a *Muc1* promoter fragment stretching from -715 to +33 (*Muc1* -715) (B, D). Luciferase activity was measured 24 to 48 h posttransfection and normalized to  $\beta$ -galactosidase activity of a cotransfected CMV-*lacZ* construct. (A, B) The indicated combinations of PPARs and RXR $\alpha$  were cotransfected with the reporters in the absence or presence of 1  $\mu$ M rosiglitazone (rosi) as labeled. The canonical PPRE reporter responds strongly to endogenous PPAR $\gamma$ , while the *Muc1* promoter requires transfection of both PPAR $\gamma$  and RXR $\alpha$  into the cells. (C, D) RXR $\alpha$  was cotransfected alone or with each of the PPARs in the absence or presence of ligands (1  $\mu$ M LG268, 5  $\mu$ M Wy-14,643, 1  $\mu$ M rosiglitazone, and 1  $\mu$ M cPGI for RXR alone, PPAR $\alpha$ , PPAR $\gamma$ , and PPAR $\delta$ , respectively). The canonical PPRE reporter responds to all three PPARs (see inset for enhanced PPAR $\delta$  data), while the *Muc1* promoter is entirely refractory to PPAR $\alpha$  and PPAR $\delta$ .

PPAR $\gamma$  or RXR $\alpha$  express intermediate levels of *Muc1* (Fig. 1A, lanes 3 and 4, and 1B, lane 2), suggesting that *Muc1* expression is directly proportional to the amount of PPAR $\gamma$ -RXR $\alpha$  heterodimers in trophoblasts.

**A PPAR $\gamma$  agonist stimulates *Muc1* induction in murine trophoblast stem cells.** TS cells proliferate and retain stem cell status as long as they are supplemented with FGF4, heparin, and embryonic fibroblast conditioned medium (29). Once the additives are withdrawn, these cells undergo terminal differentiation, as manifested by the induction of the spongiotrophoblast-specific marker 4311 4 days later (Fig. 2A, lanes 5 and 9). While PPAR $\gamma$  is only minimally expressed in proliferating TS cells, it is dramatically induced with the onset of differentiation (Fig. 2B, lanes 1 to 5), recapitulating its association with trophoblast differentiation in the intact placenta (3). Interestingly, rosiglitazone treatment of differentiated TS cells attenuates PPAR $\gamma$  expression (Fig. 2B, compare lanes 6 through 9 to lanes 2 through 5), suggesting that PPAR $\gamma$  engages in negative autoregulation.

*Muc1* expression is detected in TS cells 3 days after the onset of differentiation (Fig. 2C, lane 4). When rosiglitazone is ad-

ministered throughout differentiation, *Muc1* is still induced only at the third day of differentiation but much more robustly (Fig. 2C, lanes 8 and 9), consistent with the notion of responsiveness to PPAR $\gamma$ . In contrast, if TS cells were allowed first to differentiate for 4 days, *Muc1* can be induced as early as 4 h after rosiglitazone administration (Fig. 2E, lane 5); *Muc1* transcripts continue to accumulate in predifferentiated TS cells for at least 48 h following ligand treatment (Fig. 2E, lanes 6 and 7; also data not shown). These observations suggest that *Muc1* responds directly to liganded PPAR $\gamma$  in differentiated TS cells and that its failure to express prior to the third day of differentiation likely reflects delayed acquisition of transcriptional competence rather than a slow or indirect response to PPAR $\gamma$ .

**Robust activation of the *Muc1* promoter by PPAR $\gamma$ .** The *Muc1* promoter was next characterized for response to PPAR $\gamma$  by reporter assays with CV1 cells. As shown previously (10), multimerized consensus PPAR response elements (3xDR1) respond readily to rosiglitazone in CV-1 cells in both the absence and presence of cotransfected RXR $\alpha$  and PPAR $\gamma$  (Fig. 3A). In contrast, the proximal *Muc1* promoter (-715 to +33, with +1 denoting the 5' end of *Muc1* mRNA) required cotransfection of

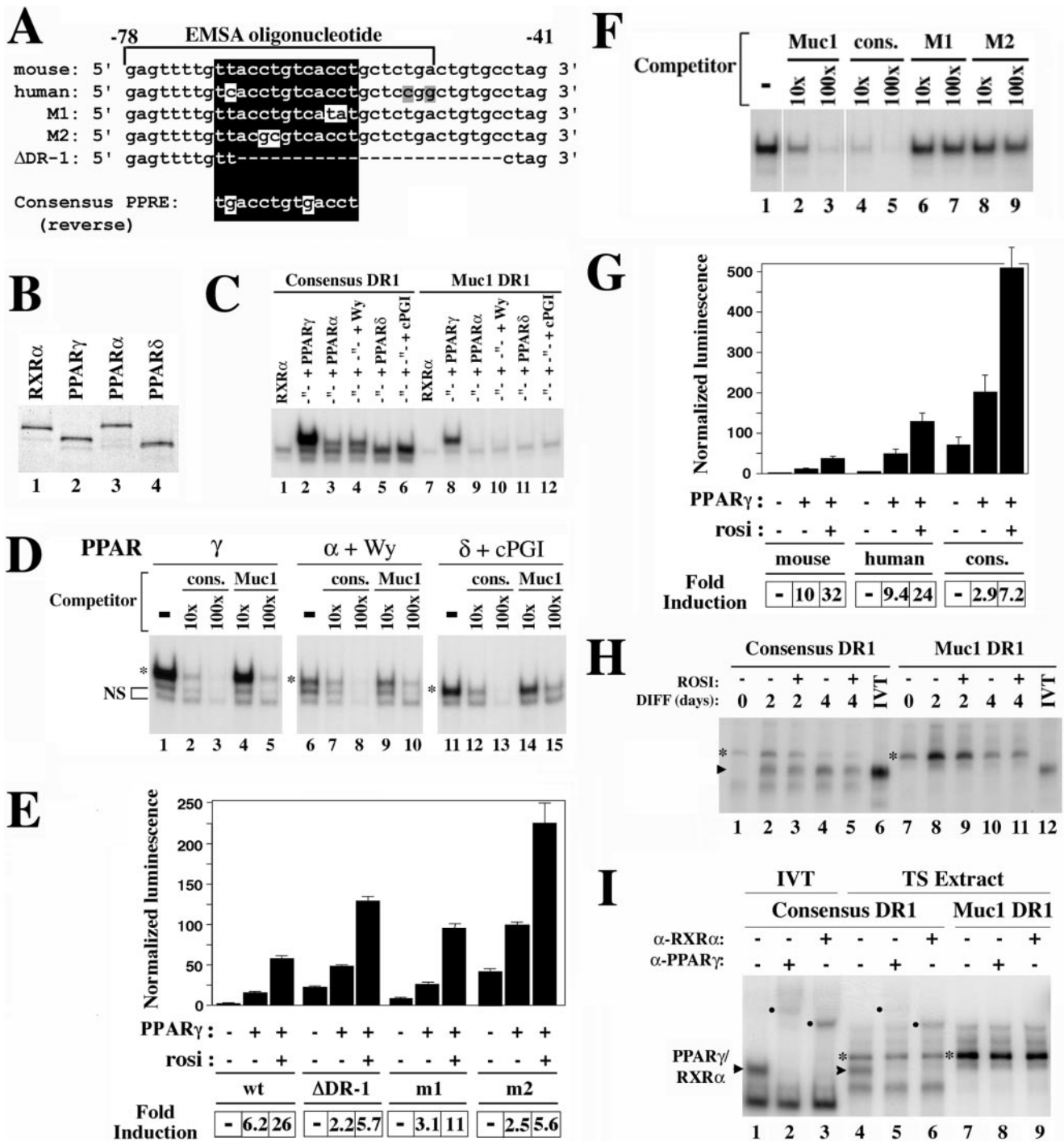


FIG. 4. A PPAR $\gamma$  binding site in the proximal *Muc1* promoter mediates basal repression. (A) Sequence alignment of mouse and human *Muc1* promoter sequences, highlighting the reverse DR1 element at the -65 position (boxed). Sequences shown are identical to the plus strand of oligonucleotides used in panels C to E and H. The consensus PPRE sequence is aligned at the bottom. M1, M2,  $\Delta$ DR-1 are the mutations introduced experimentally into the sequence in the context of either oligonucleotide probes or full promoter constructs. Equal quantities of in vitro-translated PPARs (B) were mixed with RXR $\alpha$  and used to shift oligonucleotide probes containing the *Muc1* -78 $\rightarrow$ -51 promoter sequence with either a consensus PPRE core or the native mouse *Muc1* DR1 element (C). RXR $\alpha$ -PPAR $\alpha$  or - $\delta$  heterodimers were used either without or with their cognate ligands (lanes 3 to 6 and 9 to 12), which reportedly improve DNA binding (10). (D) Complexes of RXR $\alpha$ -PPAR heterodimers with labeled consensus oligonucleotide were competed with 10 $\times$  and 100 $\times$  molar unlabeled excess of either the same oligonucleotide or the native *Muc1* DR1 sequence. A tenfold excess of the consensus probe (lanes 2, 7, and 12) competes for any of the PPARs as effectively as a 100-fold excess of native *Muc1* DR1 (lanes 5, 10, and 15), consistent with a  $\sim$ 10-fold-lower affinity of *Muc1* DR1 compared to that of consensus PPRE towards any of the PPARs. NS, nonspecific gel-shift activity. (E) Basal and PPAR $\gamma$ -induced activities of mouse *Muc1* -715 reporter fragments containing the original DR1 sequences, deletion of DR1 ( $\Delta$ DR-1), or two mutations (M1 and M2; see panel A). All transfections include CMV-*lacZ*, RXR $\alpha$ , and the respective reporter plasmid, with PPAR $\gamma$  and PPAR $\gamma$  plus rosiglitazone as variables. Fold induction, ratio of reporter activity to its activity with RXR $\alpha$  alone. (F) Complexes of RXR $\alpha$ -PPAR $\gamma$  with labeled native *Muc1* oligonucleotide were competed with 10 $\times$  and 100 $\times$

both PPAR $\gamma$  and RXR $\alpha$  to induce strong reporter activity (Fig. 3B). Unlike 3xDR1, *Muc1* was induced weakly, albeit significantly, by PPAR $\gamma$ -RXR $\alpha$  even in the absence of an exogenous agonist (three- to fivefold in different experiments), and 1  $\mu$ M rosiglitazone augmented its activity by an additional three- to fivefold (Fig. 3B). Similar response patterns and magnitudes were exhibited by fragments stretching from the +33 position to as far as -1836 or as near as the -535 position (data not shown). Thus, the proximal 535 bp of the *Muc1* promoter contain sequence information that is necessary and sufficient for activation by PPAR $\gamma$ . In aggregate, the data presented thus far provide genetic, pharmacological, and transcriptional evidence that *Muc1* is a primary PPAR $\gamma$  target gene.

**The *Muc1* promoter is refractory to PPAR $\alpha$  and PPAR $\delta$ .** The distinct biological functions of PPAR $\alpha$ , - $\gamma$ , and - $\delta$  (14) imply that each must have at least some unique transcriptional targets. However, the promoters of PPAR targets identified so far, such as acyl-coenzyme A oxidase, aP2, lipoprotein lipase, CD36, LXR $\alpha$ , and ADRP, are at least in part responsive to more than one PPAR. This pan-specificity is exemplified by the 3xDR1 reporter, which is activated by any of the PPARs in the presence of their corresponding ligands, as shown previously and reiterated here (10) (Fig. 3C). In contrast, the *Muc1* promoter is induced solely by PPAR $\gamma$  and is entirely refractory to either free or ligand-bound PPAR $\alpha$  and PPAR $\delta$  (Fig. 3D). The lack of compensatory activation of the *Muc1* promoter by PPAR $\alpha$  and PPAR $\delta$  is unique so far among established PPAR targets but is consistent with the cessation of *Muc1* expression in PPAR $\gamma$  null placentas despite ongoing expression of the two other PPARs (data not shown).

**A DR1 element in the proximal *Muc1* promoter is a low-affinity PPAR $\gamma$ -binding site.** To understand how *Muc1* is regulated by PPAR $\gamma$ , we first scanned its promoter for potential PPAR response elements (PPREs). A reverse DR1 sequence (5' AGGTGA C AGGTAA 3'; Fig. 4A) was found ~65 bp upstream of the murine *Muc1* transcription start site. The orthologous human *Muc1* promoter sequence is highly similar (5' AGGTGA C AGGTGA 3') (17). A synthetic oligonucleotide duplex spanning the *Muc1* DR1 was bound by a combination of in vitro-translated PPAR $\gamma$  and RXR $\alpha$  (Fig. 4C, lane 8) but not by RXR $\alpha$  or PPAR $\gamma$  alone (lane 7; also data not shown). However, combinations of RXR $\alpha$  with similar quantities of either PPAR $\alpha$  or PPAR $\delta$  (see Fig. 4B) exhibited only residual binding to the same sequence (Fig. 4C, lanes 9 to 12). Reverting the DR1 sequence to a consensus PPRE sequence (5' AGGTCA C AGGTCA 3') within the *Muc1* promoter sequence context significantly improved PPAR $\gamma$ -RXR $\alpha$  binding (Fig. 4C, lane 2) and restored ligand-stimulated binding of PPAR $\alpha$ -RXR $\alpha$  and PPAR $\delta$ -RXR $\alpha$  (lanes 3 to 6). Template competition experiments demonstrated that a 10-fold excess of unlabeled consensus DR1 competed for binding to any of the PPAR-RXR $\alpha$  heterodimers as effectively as a 100-fold excess

of native *Muc1* DR1 (Fig. 4D, compare lanes 5 to 2, 10 to 7, and 15 to 12). Thus, the two-base variation of the *Muc1* PPRE compromises its affinity towards all three PPARs equally; its poor interaction with PPAR $\alpha$  and PPAR $\delta$  simply reflects their lower inherent DR1 binding potential relative to that of PPAR $\gamma$  (Fig. 4C, compare lanes 4 and 6 to lane 2).

**The proximal DR1 element mediates basal silencing of *Muc1*.** To examine the role of the proximal DR1 element in the response of *Muc1* to PPAR $\gamma$ , we assayed a series of reporter constructs, where this element was inactivated by various mutations in the context of the -715 $\rightarrow$ +33 promoter fragment (Fig. 4A). Surprisingly, basal *Muc1* promoter activity was increased by either complete deletion of the DR1 or point mutations to either of its halves (Fig. 4E), both of which completely eliminated PPAR $\gamma$  binding (Fig. 4F). Although activities of DR1-deficient promoter mutants in the presence of PPAR $\gamma$  and rosiglitazone were moderately higher than that of the native *Muc1* promoter, the overall effect of PPAR $\gamma$  was significantly blunted (Fig. 4E, bottom [fold induction]). These results demonstrate that *Muc1* DR1 harbors a basal repressor, and *Muc1* expression depends in part on derepression of this element by PPAR $\gamma$ . This dependence can be alleviated by eliminating basal repression at the outset.

The human DR1 ortholog (5' AGGTGA C AGGTGA 3') retained robust response to PPAR $\gamma$  despite a threefold increase in basal activity (Fig. 4G), demonstrating that *Muc1* DR1 is functionally conserved during evolution. In contrast, altering *Muc1* DR1 into a consensus PPRE increased basal promoter activity by ~50-fold, and while maximal activity in the presence of liganded PPAR $\gamma$  was 12-fold higher than that of the native *Muc1* promoter, the response differential was blunted from 32 $\times$  to 7.2 $\times$  over the basal level (Fig. 4G). Thus, the deviation of *Muc1* PPRE from the consensus is critical for basal repression and in turn for tighter dependence of *Muc1* on PPAR $\gamma$ -mediated derepression, albeit at the expense of maximal expression.

DR1 sites are established repression targets for members of the COUP-TF family of orphan nuclear receptors (32). However, while COUP-TFs bind to a consensus DR1, none bound to the *Muc1* variant (data not shown). Moreover, cotransfection of COUP-TFI and -II did not further repress basal or PPAR $\gamma$ -dependent activity of the *Muc1* promoter (data not shown), suggesting that repression of *Muc1* DR1 is mediated by a different factor. To test whether trophoblasts contain activities that correlate with the basal DR1 repression activity from CV1 cells, electromobility shift assays were carried out with extracts of TS cells at various stages of differentiation. Two major DNA-binding activities were observed (Fig. 4H and I). The first activity interacted readily with consensus PPRE and substantially less with *Muc1* DR1. It was identified as endogenous PPAR $\gamma$ -RXR $\alpha$  heterodimers by mobility that was identical to that of in vitro-translated PPAR $\gamma$ -RXR $\alpha$ , relative

molar unlabeled excess of either the same oligonucleotide, PPRE consensus, or M1 and M2 mutant oligonucleotides (see panel A). M1 and M2 fail to compete at up to 100 $\times$  molar excess. (G) Activities of reporters with human *Muc1* DR1 or a PPRE consensus. Conditions are as for panel E. (H, I) EMSA of consensus and *Muc1* DR1 probes with extracts of TS cell differentiated for the indicated durations with or without rosiglitazone. IVT, in vitro-translated PPAR $\gamma$ /RXR $\alpha$ . Arrowheads, RXR $\alpha$ -PPAR $\gamma$ -probe complexes (H, lanes 1 to 6 and 12; I, lanes 1 and 4) that are shifted by antibodies to either PPAR $\gamma$  or RXR $\alpha$  (I, filled circles, lanes 2 and 5 and lanes 3 and 6, respectively). Asterisk, endogenous DNA-binding activity with preference for *Muc1* DR1 over consensus PPRE sequence.

abundance which mirrored PPAR $\gamma$  expression during TS cell differentiation (see Fig. 2), and full attenuation by either anti-PPAR $\gamma$  or anti-RXR $\alpha$  antibodies (Fig. 4I, lanes 5 and 6). Most importantly, the extracts contained an additional DNA-binding activity, which migrated slower than PPAR $\gamma$ -RXR $\alpha$  heterodimers and was refractory to antibodies against either receptor (Fig. 4H, lanes 1 to 5 and 7 to 11; Fig. 4I, lanes 4 to 9, asterisks). This activity exhibited marked preference towards *Muc1* DR1 over the consensus PPRE counterpart, similar to the basal repression pattern in CV1 cells. It peaked at the second day of differentiation, declining by the fourth; a repressor with such a temporal profile would potentially account for the delay in *Muc1* expression until later in differentiation despite the earlier induction of PPAR $\gamma$  (see Fig. 2). These observations correlate *Muc1* DR1-binding activity from TS cells to basal silencing activity in CV1 cells.

**Induction of *Muc1* by PPAR $\gamma$  requires both the DR1 motif and a composite enhancer element.** Although DR1 mutations blunted the response of the *Muc1* promoter to PPAR $\gamma$ , a considerable response was nevertheless retained, implicating additional elements in coregulating *Muc1* with PPAR $\gamma$ . This notion was confirmed by a series of successive 5' truncations of the promoter. Fragments extending from as near as  $-76$  or as far as  $-512$  to  $+33$ , all containing an intact DR1 element, exhibited a markedly compromised response to PPAR $\gamma$  (Fig. 5A; also data not shown). Finer truncation experiments (data not shown) narrowed the critical element to a 56-bp sequence between positions  $-535$  and  $-480$  (56U) (Fig. 5B). Systematic point mutations along the entire length of this element (data not shown), as well as partial truncations (e.g., the  $-531 \rightarrow +33$  fragment in Fig. 5A), caused only partial loss of the response to PPAR $\gamma$ , suggesting that 56U comprises several additive enhancer modules.

When placed directly upstream of the basal *Muc1* promoter, the 56U element drove robust luciferase expression (Fig. 5C) (56U/ $-45$ ), indicating that it docks an endogenous transcriptional activator present constitutively in the cells. Although not harboring a recognizable PPRE, the 56U/ $-45$  promoter construct still displayed modest three- and sixfold responses to free and ligand-stimulated PPAR $\gamma$ , respectively (Fig. 5C). However, placing the 56U element upstream of a 108-bp proximal *Muc1* promoter fragment that includes the DR1 motif (56U/ $-108$ ) restored basal silencing and in turn an  $\sim 70$ -fold response to ligand-activated PPAR $\gamma$ . These analyses indicate that regulation of the *Muc1* promoter by PPAR $\gamma$  is mediated cooperatively by two distinct elements, a low-affinity PPRE that serves as a basal silencer at  $\sim -65$  and a composite enhancer at  $-500$ . Each of these elements is modestly responsive to PPAR $\gamma$  on its own, and together they control a robust and specific response to PPAR $\gamma$ .

**Analogous localization of MUC1 in the placenta and luminal epithelia.** The MUC1 protein is localized to the apical-luminal surface of simple secretory epithelia, such as the milk ducts of the mammary gland (5, 19), as shown in Fig. 6A. To understand the biological significance of MUC1 expression in the placenta, we sought to determine whether it is localized in this organ to a comparable luminal structure.

Figures 6C and D demonstrate that the maternal lacunae in the labyrinth qualify as a lumen analog. Placental MUC1 is confined to the apical surface of layer I trophoblasts in the labyrinth, surrounding the lacunae, and is absent from the fetal endothe-

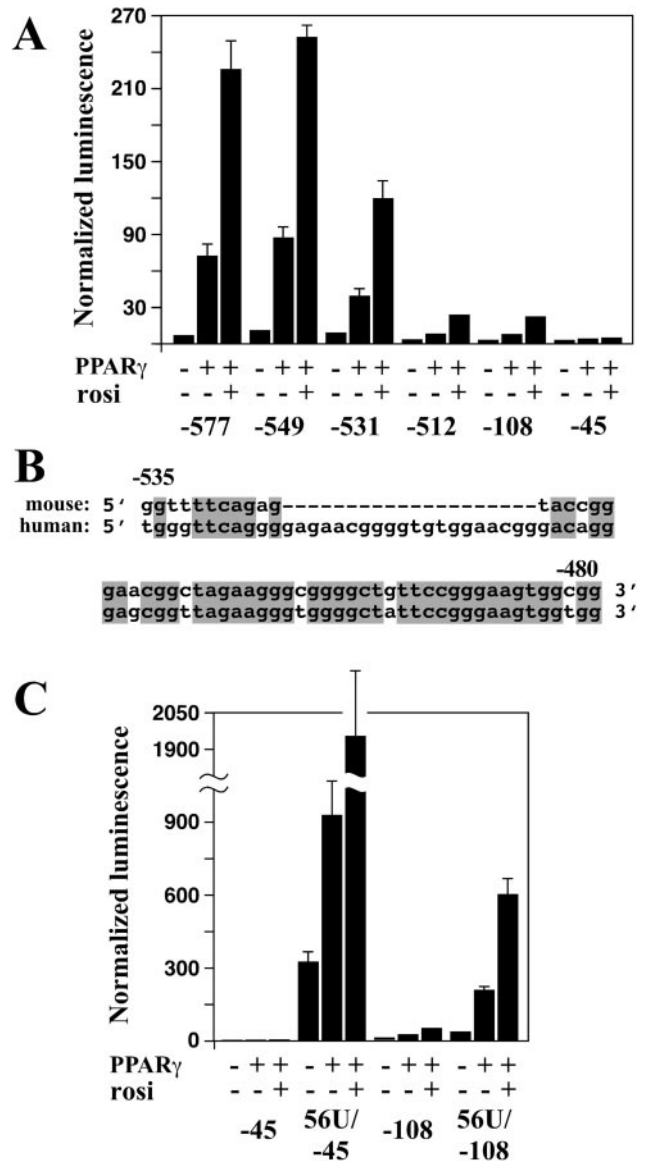


FIG. 5. A 56-bp upstream element mediates the PPAR $\gamma$  response of the *Muc1* promoter. (A) Truncation analysis of the *Muc1* promoter. Numbers indicate 5' termini of each fragment relative to the transcription start site. All fragments stretch to the  $+33$  position of the *Muc1* gene. (B) Nucleotide sequence of the murine 56-bp upstream element (56U) element, aligned with its human ortholog. Gray boxes mark mouse-human homologies. Note the apparent insertion within the human sequence. (C) Basal and PPAR $\gamma$ -dependent activities of "abbreviated" *Muc1* promoter constructs. The 56U element was appended directly to either the basal  $-45$  promoter fragment or the DR1-containing  $-108$  one. Resulting reporter activities were compared to those of the corresponding  $-45$  and  $-108$  control fragments. Note the different scale compared to that for panel A.

lium, as well as layer II or III cells and the spongiotrophoblast. The immunofluorescent signal is absent from placentas of *Muc1*<sup>-/-</sup> embryos (Fig. 6E and F), confirming that the signal observed in wild-type placentas is specific to MUC1. Double immunofluorescence with anti-caveolin 1 antibodies, whose presence in the placenta is confined to the fetal endothelium, further demonstrates that MUC1 completely segregates to the maternal interface of the placenta (Fig. 6G). Thus, the maternal blood

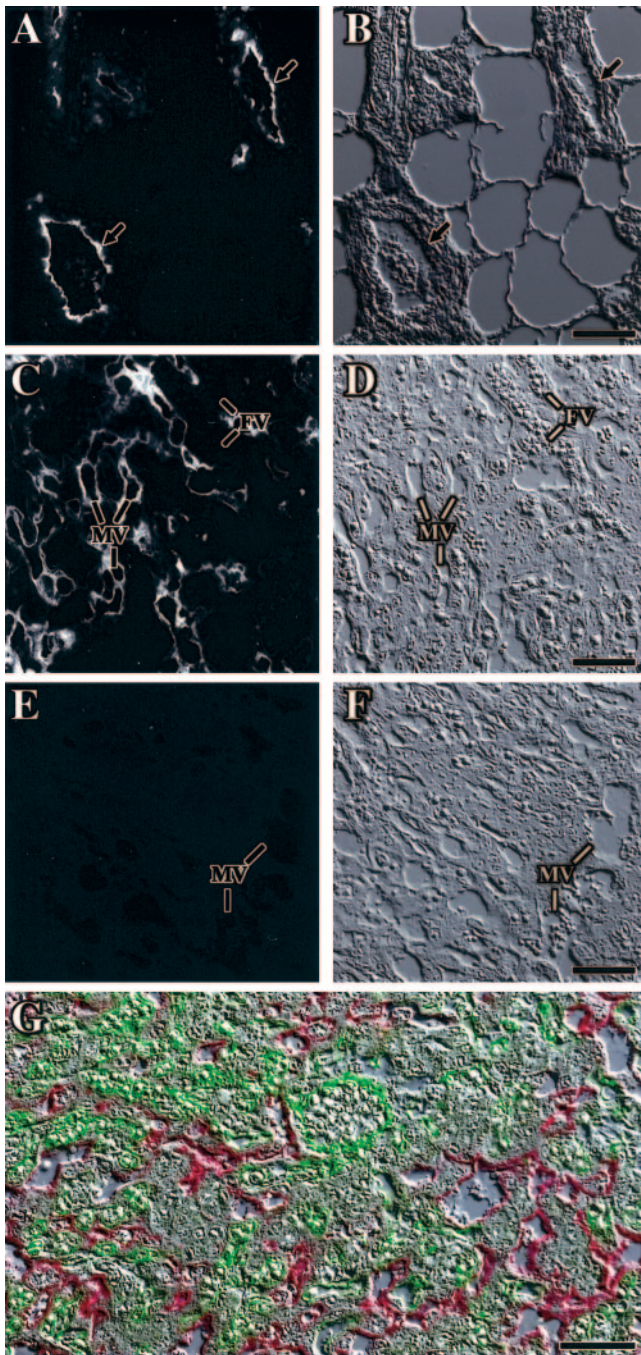


FIG. 6. MUC1 is localized to the trophoblast lining of maternal blood pools in the placenta. Paraffin sections of mammary glands (A, B) and E11.5 placentas (C to F) were probed with anti-MUC1 monoclonal antibody and a cy3-conjugated secondary antibody. In the pregnant mammary gland, MUC1 is restricted to the luminal surface of milk ducts (arrows in panels A and B). In the placental labyrinth (C, D), MUC1 is localized exclusively to the apical surface of layer I trophoblasts, surrounding the maternal blood pools (MV), and is not associated with fetal blood vessels (FV). Signal specificity is confirmed by its absence in placentas of *Muc1*<sup>-/-</sup> littermates (E, F). (A, C, and E) Fluorescence; (B, D, and F) corresponding Nomarski images. Scale bars, 50  $\mu$ m. (G) Coimmunofluorescence with anti-MUC1 antibodies (red) and anti-caveolin-1 antibodies (green). Caveolin-1 is confined to the fetal endothelium and exhibits no signal overlap with MUC1, demonstrating the complete sequestration of MUC1 to the maternal side of the labyrinth. Scale bar, 50  $\mu$ m.

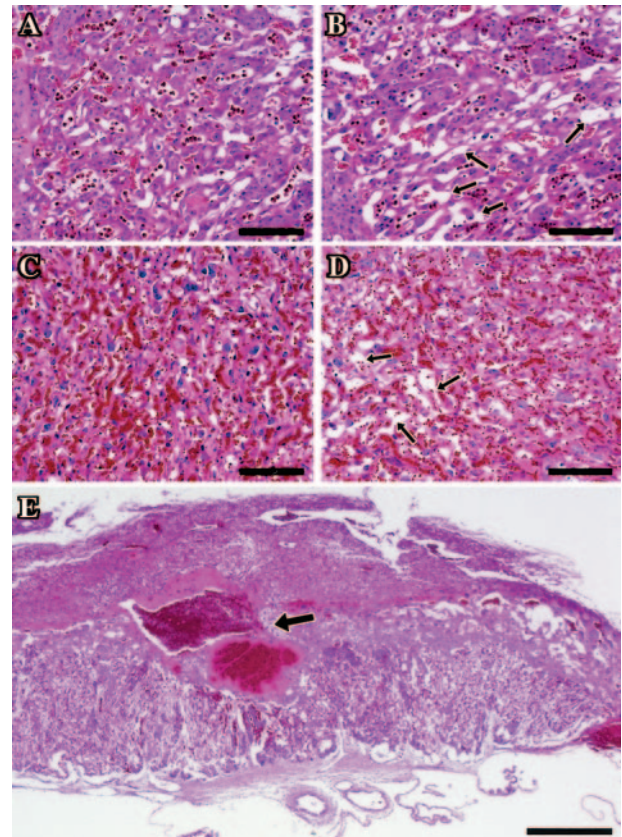


FIG. 7. Maternal blood pool defects in *Muc1*<sup>-/-</sup> placentas. (A to D) Hematoxylin and eosin-stained paraffin section of wt (A, C) and *Muc1*<sup>-/-</sup> labyrinths (B, D) at E12.5 (A, B) and E18.5 (C, D). Arrows point to dilated maternal lacunae within the mutant placentas. Note that the more dilated spaces in the E12.5 wt placenta (A) are mostly fetal blood vessels containing nucleated erythrocytes. Fetal vessel space is actually shrunken in the *Muc1*<sup>-/-</sup> placenta (B), perhaps due to excessive space allocation to the dilated maternal lacunae. Scale bars, 100  $\mu$ m. (E) A hematoxylin- and eosin-stained E14.5 *Muc1*<sup>-/-</sup> placenta. Arrow points to a massive hemorrhage at the interface of the labyrinth and the spongiotrophoblast. Scale bar, 500  $\mu$ m.

pools in the placenta share anatomical properties with secretory lumens, and by inference, PPAR $\gamma$  emerges as a potential common regulator of these analogous properties.

**Low-penetrance maternal vascular defects in the *Muc1* null labyrinth.** We next assessed the contribution of PPAR $\gamma$  by histological analysis of *Muc1* null placentas. The normal Mendelian distribution and birth size, as well as the full viability of *Muc1* null pups (26), provided no prior evidence of defects in *Muc1* null placentas. Our analyses confirmed this notion, although detailed histological inspection revealed minor dilations and tears in the maternal lacunae of  $\sim$ 50% of *Muc1* null placentas between E12.5 and E18.5 (Compare Fig. 7B and D to Fig. 7A and C, respectively). Two out of nineteen *Muc1* null placentas, but none of the wild-type placentas, exhibited expansive thrombi (see Fig. 7E), which could represent harsher manifestations of the same defect. Association of these defects with the maternal lacunae is consistent with the localization of MUC1 to layer I of the labyrinth, around these lacunae. Thus, MUC1 may cooperate with additional targets downstream of

PPAR $\gamma$  to maintain the integrity of maternal blood pools, which are severely torn and hemorrhagic in PPAR $\gamma$  null placentas (3). All other PPAR $\gamma$ -dependent histopathies, including labyrinthine trophoblast differentiation, fetal vessel permeation, and lipid droplet accumulation, were normal in *Muc1* null placentas (data not shown). These last functions are likely regulated by other PPAR $\gamma$  target genes.

## DISCUSSION

Here we use gene-targeted mice as a differential platform in order to understand the molecular functions of PPAR $\gamma$  in embryonic development. Our studies identify the *Muc1* gene as a PPAR $\gamma$  target in trophoblasts, reveal a novel combinatorial mechanism of gene regulation by PPAR $\gamma$ , and implicate PPAR $\gamma$  in regulating epithelial functions of trophoblasts. Importantly, *Muc1* is the only direct PPAR $\gamma$  target so far with no obvious ties to lipid or energy metabolism, demonstrating the versatile, nonredundant functions of this nuclear receptor in different biological systems.

**Novel insights into gene regulation by PPAR $\gamma$ .** The dependence of *Muc1* expression on PPAR $\gamma$  is manifested in every regulatory parameter tested. These include the complete shutdown of *Muc1* expression in PPAR $\gamma$  null placentas, its strong upregulation by an agonist in TS cells, and the robust PPAR $\gamma$ -specific response of its promoter. *Muc1* thus provides a new, biologically relevant template for mechanistic studies of PPAR $\gamma$ -regulated transcription.

Before discussing the details of *Muc1* regulation by PPAR $\gamma$ , it is important to address the issue of cell type specificity. Because *Muc1* is not expressed in all PPAR $\gamma$ -expressing tissues, most notoriously adipocytes or macrophages (data not shown), it is clear that its regulation by PPAR $\gamma$  in trophoblasts is tissue specific. Therefore, the activation of its promoter in kidney-derived CV1 cells is surprising. However, this activation is robust, specific for PPAR $\gamma$  over PPAR $\alpha$  and PPAR $\delta$ , and involves complex interactions between two *cis* regulatory elements, arguing that it is neither coincidental nor promiscuous. Most importantly, a DNA binding activity from TS cells (Fig. 4H and I), whose preference for *Muc1* DR1 over consensus PPRE mirrors that of the basal silencing activity in CV1 cells, suggests that components of the *Muc1* regulatory network are likely shared between trophoblasts and CV1 cells. In hindsight, the ability of CV1 cells to support the *Muc1* response to PPAR $\gamma$  may not be as surprising, considering their reported renal epithelial origin (13) and the notion that emerges here of molecular and cellular similarities between trophoblasts and epithelia.

The response of *Muc1* to PPAR $\gamma$  is an interplay between two *cis* elements: a direct repeat sequence (DR1) that comprises a variant PPRE and a composite 56-bp-wide enhancer (56U). The 56U element drives robust transcription independently of PPAR $\gamma$ , suggesting that it constitutively docks active transcription factors. However, in the basal state, such as in undifferentiated trophoblasts or nontransfected cells, PPAR $\gamma$  is absent, and the DR1 element dominantly silences the promoter.

PPAR $\gamma$ -RXR $\alpha$  heterodimers can bind the variant DR1, albeit with a 10-fold-lower affinity than consensus PPRE. The affinity of RXR $\alpha$ -PPAR $\alpha$  and RXR $\alpha$ -PPAR $\delta$  heterodimers is reduced similarly, suggesting that preferential activation of *Muc1* by PPAR $\gamma$  is likely not due to deviation from the consensus.

Mutating the DR1 motif not only increases basal *Muc1* promoter activity but significantly attenuates the response differential, indicating that PPAR $\gamma$  regulates derepression of this element. Surprisingly, when canonical PPRE is restored in place of the original DR1, basal repression is lost and the degree of response to PPAR $\gamma$  is blunted. Thus, silencing and temporally controlled PPAR $\gamma$ -mediated derepression are critical for *Muc1* regulation and require modification of the PPRE sequence. However, cell type specificity and expression intensity must be provided elsewhere. We hypothesize that this crucial biological context for *Muc1* induction, as well as its remarkably specific response to PPAR $\gamma$ , are mediated by the 56U element, where an epithelium-specific enhancer has been previously characterized (1, 16, 23, 24).

One means of achieving transcriptional cooperativity between the 56U and DR1 elements is for a constitutive, tissue-specific 56U-bound transcription complex of factors and cofactors to tether PPAR $\gamma$ -RXR heterodimers to the *Muc1* promoter. Ligands increase the interaction of PPAR $\gamma$  with various coactivators and could accordingly enhance cooperativity by recruiting PPAR $\gamma$  to an integral coactivator component of the 56U-bound complex. Such model would explain the puzzling ability of PPAR $\gamma$  and rosiglitazone to directly activate the 56U element (see Fig. 5C, 56U/45). Tethering through 56U should in turn greatly facilitate interaction of the PPAR $\gamma$ -RXR heterodimer with its low-affinity DR1 target, which would further cement an active transcription complex on the *Muc1* promoter. This model envisions PPAR $\gamma$  agonists as mediators of cooperativity between promoter elements, and hence in the control of transcriptional context and specificity, beyond their known role as transcriptional pacemakers.

The combinatorial complexity of *Muc1* regulation by PPAR $\gamma$  has not been documented previously with other PPAR $\gamma$ -regulated promoters. Future studies should reveal whether this form of regulation is unique to *Muc1* or whether it has simply been overlooked heretofore.

**PPAR $\gamma$ , MUC1, and the analogies between trophoblast and epithelia.** The identification of *Muc1*, a classical marker of luminal epithelia, as a PPAR $\gamma$  target in trophoblasts suggests an analogy between the placenta and prototypic luminal epithelia. In the placenta, MUC1 is confined exclusively to the apical surface of the labyrinth, surrounding the lacunae that conduct maternal blood. This pattern reiterates the luminal localization of MUC1 in prototypic glandular epithelia (5). Although glandular lumens contain gland secretions, and the placental "lumens" conduct blood, the analogous distribution of MUC1 in both highlights their architectural similarities and suggests that they share additional properties. The analogy extends to the induction of *Muc1* expression upon differentiation of the mammary gland during pregnancy and lactation (19), which resembles its induction during trophoblast differentiation. PPAR $\gamma$  is expressed abundantly in the mammary epithelium and other luminal epithelia (12, 18), and it is therefore plausible that its role in these tissues may resemble its placental function.

*Muc1* deficiency is not lethal, and does not cause classical manifestations of placental defects, such as intrauterine growth retardation. Approximately 50% of *Muc1*-deficient placentas exhibit mild structural anomalies in the maternal lacunae, which could reflect a partial role of *Muc1* down-regulation in the overt dilation and breakage seen in the lacunae of PPAR $\gamma$



null placentas (3). It is equally possible that the major function of *Muc1* downstream of PPAR $\gamma$  is nonstructural. For example, the MUC1 protein may primarily function to protect the placenta against other genetic or maternally borne insults, such as bacterial pathogens (8). The incomplete penetrance of the phenotype may reflect the variable extent or frequency of these putative insults. The full function of *Muc1* has yet to be revealed, but regardless, its elaborate regulation by PPAR $\gamma$  suggests that it is a functionally important target rather than a coincidental one. At the same time, the mild *Muc1* null phenotype implies that additional targets transduce the essential developmental signals of PPAR $\gamma$  in the placenta.

This study finds that the expression of PPAR $\gamma$  is tightly regulated in TS cells. In undifferentiated TS cells, PPAR $\gamma$  expression is minimal and is confined to rare cells that have differentiated spontaneously (immunofluorescence data [not shown]). Within hours of FGF4 and conditioned medium deprivation, PPAR $\gamma$  expression is induced dramatically in the vast majority of cells in the culture, suggesting that it is an early determinant in the differentiation of all trophoblast lineages. These observations align with the importance of PPAR $\gamma$  for trophoblast differentiation and placental development in the whole animal (3). The rapid induction of PPAR $\gamma$  in differentiating TS cells is reminiscent of its early induction during adipogenesis *in vitro* and *in vivo* (30). In contrast, *Muc1* is expressed neither in nascent nor in mature adipocytes, whereas adipogenic PPAR $\gamma$  target genes, such as aP2, CD36, LXR $\alpha$  and lipoprotein lipase, are either absent from the placenta or impervious to the status of PPAR $\gamma$  in the organ (data not shown). These differences suggest that while PPAR $\gamma$  is intimately involved in early differentiation of both trophoblasts and adipocytes, its mechanisms of action and downstream targets are distinct in each cell type.

#### ACKNOWLEDGMENTS

We thank Janet Rossant and Tilo Kunath for the TS cell line GFP-Trf and probes for 4311 and mash-2; Barbara Knowles and Karen Fancher for mammary gland sections; Greg Martin, Judy Ford, and members of the Jackson Laboratory Biological Imaging core for assistance with histology, immunofluorescence, and microscopy; Henry Juguilon for assistance with reporter assays; Timothy O'Brien and Susan Ackerman for insightful comments and discussions; Sarah Williamson for figure preparation; and Beth Whitney and Elaine Stevens for administrative assistance.

R.M.E. is an investigator of the Howard Hughes Medical Institute at The Salk Institute. This work was supported in part by NIH HD044103 to Y.B. and by CORE CA34196 to The Jackson Laboratory.

#### REFERENCES

- Abe, M., and D. Kufe. 1993. Characterization of cis-acting elements regulating transcription of the human DF3 breast carcinoma-associated antigen (MUC1) gene. *Proc. Natl. Acad. Sci. USA* **90**:282–286.
- Adamson, S. L., Y. Lu, K. J. Whiteley, D. Holmyard, M. Hemberger, C. Pfarrer, and J. C. Cross. 2002. Interactions between trophoblast cells and the maternal and fetal circulation in the mouse placenta. *Dev. Biol.* **250**:358–373.
- Barak, Y., M. C. Nelson, E. S. Ong, Y. Z. Jones, P. Ruiz-Lozano, K. R. Chien, A. Koder, and R. M. Evans. 1999. PPAR $\gamma$  is required for placental, cardiac, and adipose tissue development. *Mol. Cell* **4**:585–595.
- Berger, J., and D. E. Moller. 2002. The mechanisms of action of PPARs. *Annu. Rev. Med.* **53**:409–435.
- Braga, V. M., L. F. Pemberton, T. Duhig, and S. J. Gendler. 1992. Spatial and temporal expression of an epithelial mucin, Muc-1, during mouse development. *Development* **115**:427–437.
- Chawla, A., W. A. Boisvert, C. H. Lee, B. A. Laffitte, Y. Barak, S. B. Joseph, D. Liao, L. Nagy, P. A. Edwards, L. K. Curtiss, R. M. Evans, and P. Tontonoz. 2001. A PPAR $\gamma$ -LXR-ABCA1 pathway in macrophages is involved in cholesterol efflux and atherogenesis. *Mol. Cell* **7**:161–171.
- Cross, J. C. 2000. Genetic insights into trophoblast differentiation and placental morphogenesis. *Semin. Cell Dev. Biol.* **11**:105–113.
- DeSouza, M. M., G. A. Surveyor, R. E. Price, J. Julian, R. Kardon, X. Zhou, S. Gendler, J. Hilkens, and D. D. Carson. 1999. MUC1/episialin: a critical barrier in the female reproductive tract. *J. Reprod. Immunol.* **45**:127–158.
- Forman, B. M., P. Tontonoz, J. Chen, R. P. Brun, B. M. Spiegelman, and R. M. Evans. 1995. 15-Deoxy- $\delta$  12,14-prostaglandin J2 is a ligand for the adipocyte determination factor PPAR $\gamma$ . *Cell* **83**:803–812.
- Forman, B. M., J. Chen, and R. M. Evans. 1997. Hypolipidemic drugs, polyunsaturated fatty acids, and eicosanoids are ligands for peroxisome proliferator-activated receptors  $\alpha$  and  $\delta$ . *Proc. Natl. Acad. Sci. USA* **94**:4312–4317.
- Hubank, M., and D. G. Schatz. 1994. Identifying differences in mRNA expression by representational difference analysis of cDNA. *Nucleic Acids Res.* **22**:5640–5648.
- Jain, S., S. Pulikuri, Y. Zhu, C. Qi, Y. S. Kanwar, A. V. Yeldandi, M. S. Rao, and J. K. Reddy. 1998. Differential expression of the peroxisome proliferator-activated receptor  $\gamma$  (PPAR $\gamma$ ) and its coactivators steroid receptor coactivator-1 and PPAR-binding protein PBP in the brown fat, urinary bladder, colon, and breast of the mouse. *Am. J. Pathol.* **153**:349–354.
- Jensen, F. C., A. J. Girardi, R. V. Gilden, and H. Koprowski. 1964. Infection of human and simian tissue cultures with Rous sarcoma virus. *Proc. Natl. Acad. Sci. USA* **52**:53–59.
- Kersten, S., B. Desvergne, and W. Wahli. 2000. Roles of PPARs in health and disease. *Nature* **405**:421–424.
- Kliwer, S. A., K. Umeson, D. J. Noonan, R. A. Heyman, and R. M. Evans. 1992. Convergence of 9-cis retinoic acid and peroxisome proliferator signaling pathways through heterodimer formation of their receptors. *Nature* **358**:771–774.
- Kovarik, A., N. Peat, D. Wilson, S. J. Gendler, and J. Taylor-Papadimitriou. 1993. Analysis of the tissue-specific promoter of the MUC1 gene. *J. Biol. Chem.* **268**:9917–9926.
- Lancaster, C. A., N. Peat, T. Duhig, D. Wilson, J. Taylor-Papadimitriou, and S. J. Gendler. 1990. Structure and expression of the human polymorphic epithelial mucin gene: an expressed VNTR unit. *Biochem. Biophys. Res. Commun.* **173**:1019–1029.
- Mueller, E., P. Sarraf, P. Tontonoz, R. M. Evans, K. J. Martin, M. Zhang, C. Fletcher, S. Singer, and B. M. Spiegelman. 1998. Terminal differentiation of human breast cancer through PPAR $\gamma$ . *Mol. Cell* **1**:465–470.
- Parry, G., J. Li, J. Stubbs, M. J. Bissell, C. Schmidhauser, A. P. Spicer, and S. J. Gendler. 1992. Studies of Muc-1 mucin expression and polarity in the mouse mammary gland demonstrate developmental regulation of Muc-1 glycosylation and establish the hormonal basis for mRNA expression. *J. Cell Sci.* **101**:191–199.
- Rosen, E. D., and B. M. Spiegelman. 2001. PPAR $\gamma$ : a nuclear regulator of metabolism, differentiation and cell growth. *J. Biol. Chem.* **276**:37731–37734.
- Rossant, J., and J. C. Cross. 2001. Placental development: lessons from mouse mutants. *Nat. Rev. Genet.* **2**:538–548.
- Sapin, V., P. Dolle, C. Hindelang, P. Kastner, and P. Chambon. 1997. Defects of the chorioallantoic placenta in mouse RXR $\alpha$  null fetuses. *Dev. Biol.* **191**:29–41.
- Shirotani, K., J. Taylor-Papadimitriou, S. J. Gendler, and T. Irimura. 1994. Transcriptional regulation of the MUC1 mucin gene in colon carcinoma cells by a soluble factor. Identification of a regulatory element. *J. Biol. Chem.* **269**:15030–15035.
- Shirotani, K., and T. Irimura. 1998. Purification of nuclear proteins that potentially regulate transcription of the MUC1 mucin gene induced by a soluble factor. *J. Biochem.* **124**:585–590.
- Spicer, A. P., G. Parry, S. Patton, and S. J. Gendler. 1991. Molecular cloning and analysis of the mouse homologue of the tumor-associated mucin, MUC1, reveals conservation of potential O-glycosylation sites, transmembrane, and cytoplasmic domains and a loss of minisatellite-like polymorphism. *J. Biol. Chem.* **266**:15099–15109.
- Spicer, A. P., G. J. Rowse, T. K. Lidner, and S. J. Gendler. 1995. Delayed mammary tumor progression in Muc-1 null mice. *J. Biol. Chem.* **270**:30093–30101.
- Sporn, M. B., N. Suh, and D. J. Mangelsdorf. 2001. Prospects for prevention and treatment of cancer with selective PPAR $\gamma$  modulators (SPARMs). *Trends Mol. Med.* **7**:395–400.
- Sucov, H. M., E. Dyson, C. L. Gumeringer, J. Price, K. R. Chien, and R. M. Evans. 1994. RXR  $\alpha$  mutant mice establish a genetic basis for vitamin A signaling in heart morphogenesis. *Genes Dev.* **8**:1007–1018.
- Tanaka, S., T. Kunath, A. K. Hadjantonakis, A. Nagy, and J. Rossant. 1998. Promotion of trophoblast stem cell proliferation by FGF4. *Science* **282**:2072–2075.
- Tontonoz, P., E. Hu, and B. M. Spiegelman. 1994. Stimulation of adipogenesis in fibroblasts by PPAR $\gamma$  2, a lipid-activated transcription factor. *Cell* **79**:1147–1156.
- Wendling, O., P. Chambon, and M. Mark. 1999. Retinoid X receptors are essential for early mouse development and placentogenesis. *Proc. Natl. Acad. Sci. USA* **96**:547–551.
- Zhang, Y., and M. L. Dufau. 2004. Gene silencing by nuclear orphan receptors. *Vitam. Horm.* **68**:1–48.